Table 1: Silicon material of investigated devices.

Acronoym	Crystal type	Crystal producer	Resistivity [kΩcm]	[O] [10^{16} cm^{-3}]	[C] [10^{16} cm^{-3}]
WM-3k	n-FZ	Wacker [a)]	2.7	< 5	< 0.5
WE-7-25k	n-FZ	Wacker [a)]	10 - 20	< 5	< 0.5
WI-4k	n- FZ	Wacker [a)]	4.0	< 0.02	< 3
WI-400	n- FZ	Wacker [a)]	0.42	< 10	< 2
TS-7k	n- FZ	Topsil [b)]	6.6	< 5	< 0.5
II-800	n- FZ	ITME [c)]	0.78	17	< 2
II-120	n- FZ	ITME [c)]	0.11	< 10	2
IH-130	n-FZ	ITME [c)]	0.13	< 10	2
Cz-140	n-Cz	Polovodice [d)]	0.14	90	0.5
ID-400	p-EPI	ITME [c)]	0.4	4-20	1-2
ID-2k	p-EPI	ITME [c)]	1.6	3-20	1-2
ID-4k	p-EPI	ITME [c)]	3.9	4-60	1-2

[a)] Wacker AG, Burghausen, Germany
[b)] Topsil, Frederikssund, Denmark
[c)] Institute of Electronic Materials Technology, Warsaw, Poland
[d)] Polovodice, Prague, Czech Republic

Table 2: Parameters of current annealing at different temperatures T_a (Eq. 2). For the fit the parameter t_0 was set to 1 min.

T_a [°C]	a_0 10^{-17} *A/cm*	t_1 *min*	a_1 10^{-17} *A/cm*	a_2 10^{-18} *A/cm*
21	1.23	1.4×10^{4}	7.07	3.29
49	1.28	260	5.36	3.11
60	1.26	94	4.87	3.16
80	1.13	9	4.23	2.83
106	-	-	3.38	2.97

Table 3: Defect parameters. The given introduction rates refer to certain annealing states at 60°C: (a) after 5 min and after 82000 min, (b) annealed in the period 5min to 10000 min and (c) after anneal to 8200 min.

Defect	DE_t [eV]	s_t [cm^2]	Introduction rate [cm^{-1}]
E3	0.24	$\approx10^{-14}$	0.24→0.41 (a)
E4a	0.36	$\approx10^{-14}$	0.26 (b)
E4b	0.46	1×10^{-14}	0.62 (b)
E4	0.41	1.5×10^{-15}	1.04 (c)

Table 4:
1 MeV neutron equivalent introduction rates as measured after an annealing of 80 min at 60°C.

Particle	E2 [cm^{-1}]	E3 [cm^{-1}]	E4 [cm^{-1}]	H1 [cm^{-1}]	(E2+H1)/E4
27 MeV p	1.79	0.52	1.26	2.34	3.28
23 GeV p	1.35	0.46	1.35	1.95	2.44
192 MeV π^+	1.34	0.39	1.30	1.83	2.43
5.2 MeV n	0.82	0.30	1.38	1.14	1.42

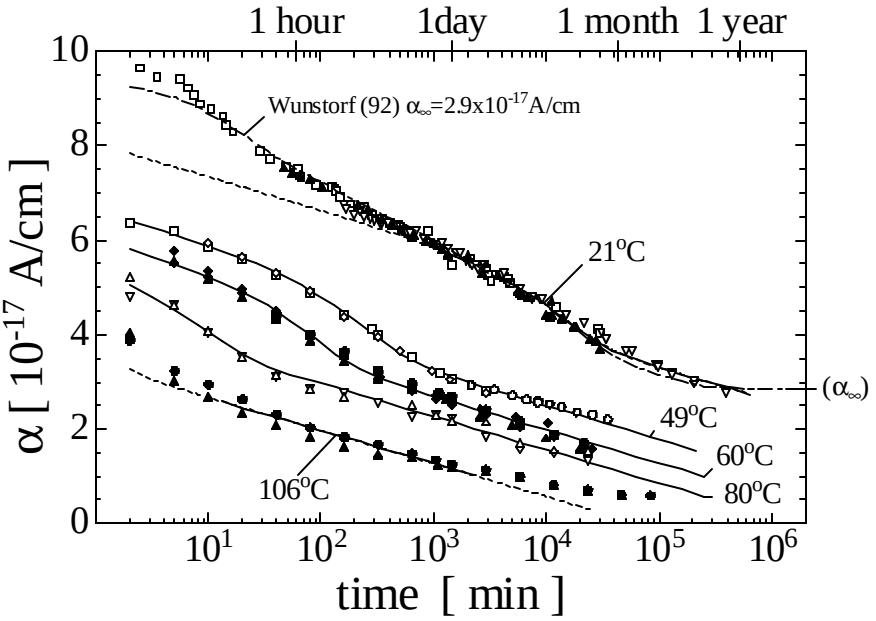

Fig 1: Current related damage rate α as function of cumulated annealing time at different annealing temperatures. Solid lines represent fits according to Eq. (2) and the dashed-dotted line a simulation according to [17]. The leakage current was measured at room temperature and corrected to 20°C.

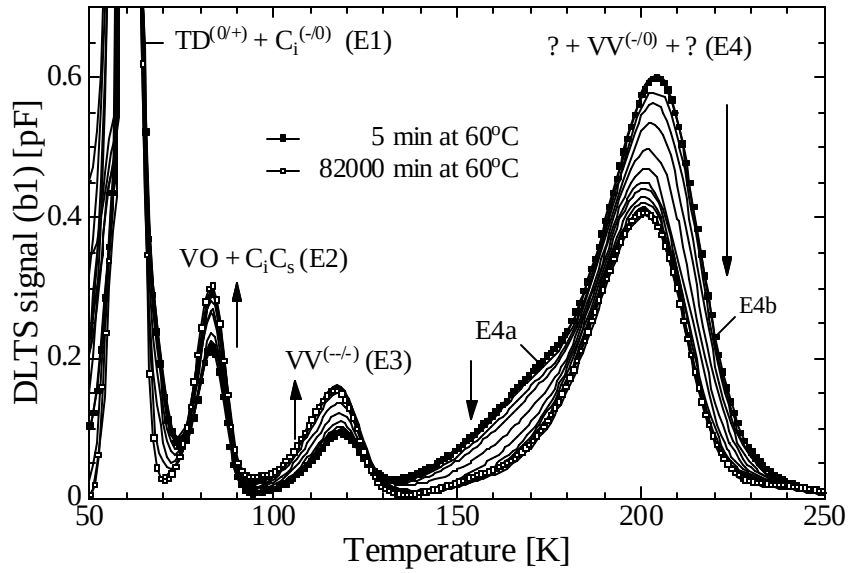

Fig.2: Evolution of the DLTS spectrum at 60°C for a neutron irradiated sample produced from Cz silicon. The main part of the huge peak at 60K (E1) is due to thermal donors (TD) observed in the material already before irradiation.

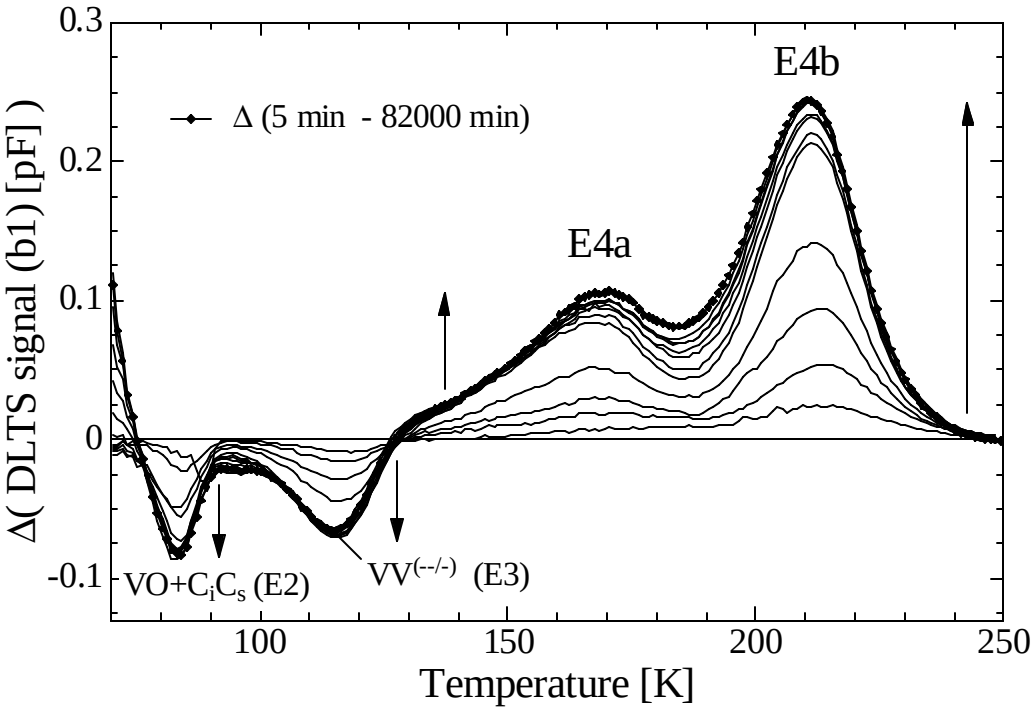

Fig. 3. Evolution of the "difference spectra" corresponding to the spectra shown in Fig.2.

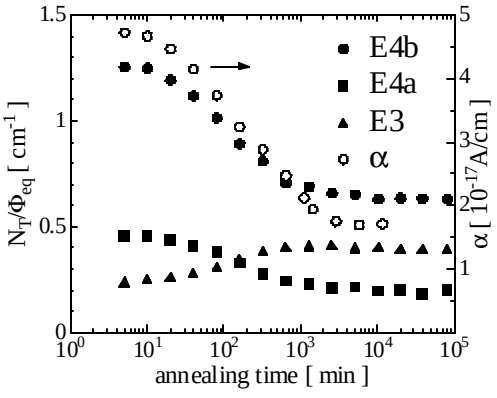

Fig.4.Annealing of defect concentration (E3, E4a, E4b) and α value (see text).

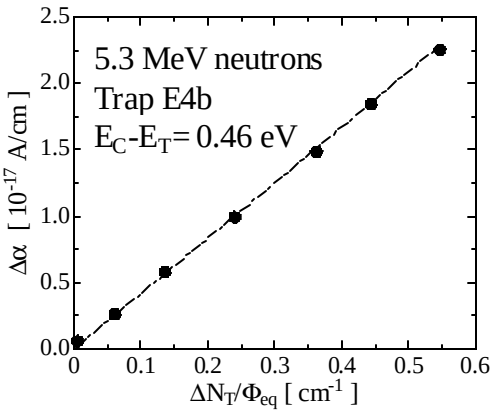

Fig.5.Correlation between trap E4b and leakage current (α value).

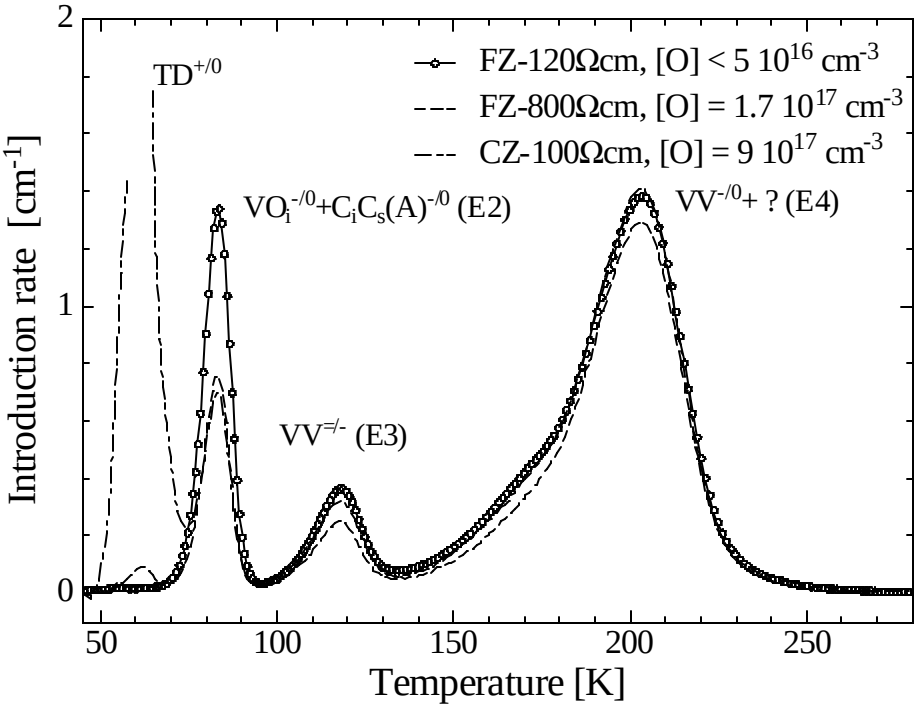

Fig. 6. DLTS spectra (normalized to introduction rate at 200K) obtained after irradiation with neutrons and a subsequent 80min heat treatment at 60°C for different materials (see legend).

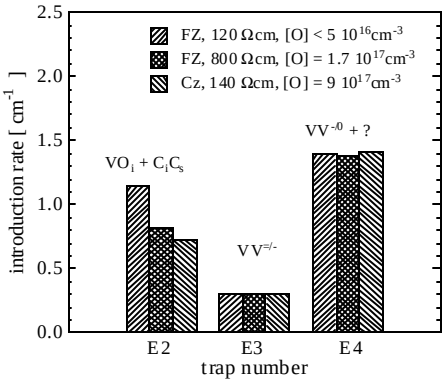

Fig.7. Material dependent introduction rates of defects E2, E3 and E4.

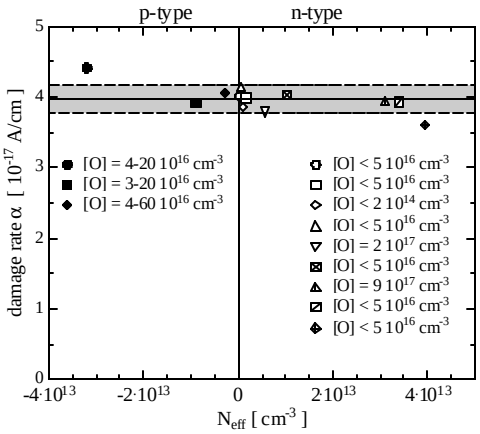

Fig. 8. Damage rate α as function of effective doping concentration.

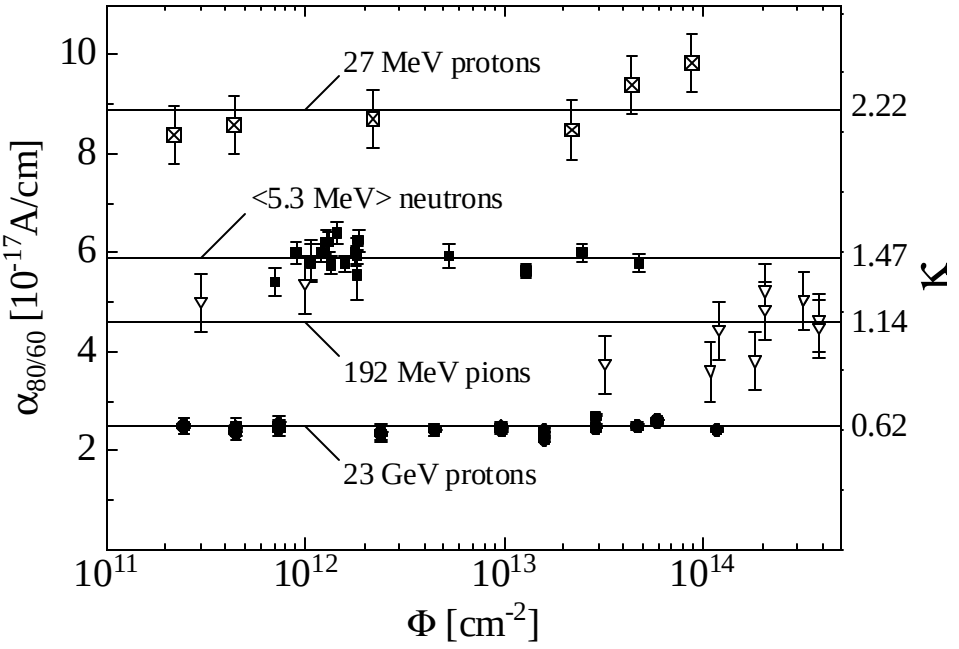

Fig. 9. α values for samples of same type irradiated with 27 MeV protons, 5.3 MeV neutrons, 192 MeV π^+ and 23 GeV protons measured after a 80min lasting heat treatment at 60°C. The scale on the right hand side indicates the corresponding experimental hardness factors κ.

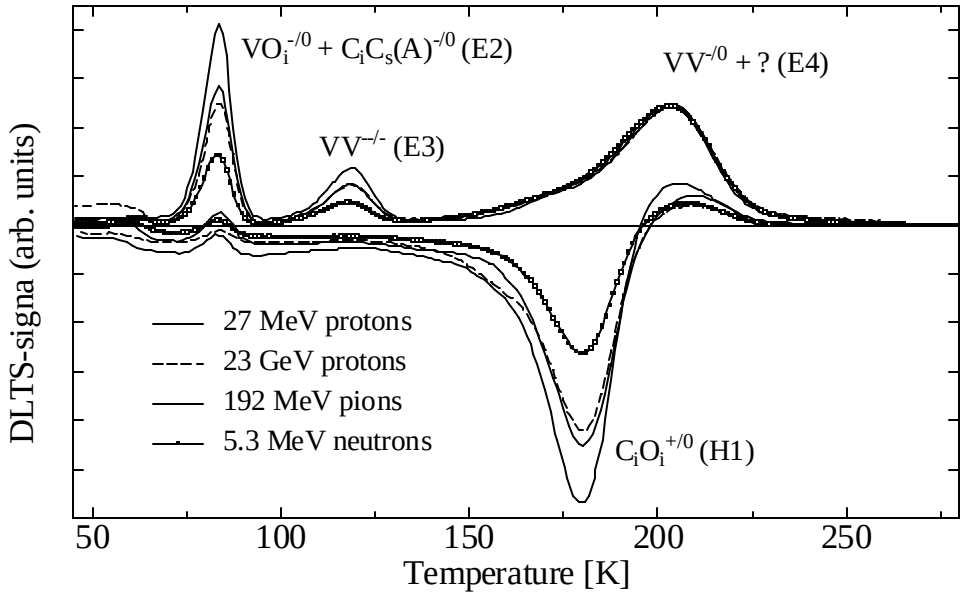

Fig. 10. DLTS spectra obtained on samples from the same wafer obtained after irradiation with different particles (see legend) and a 80min lasting heat treatment at 60°C. The spectra are scaled to superpose at the peak maximum of defect level E4.

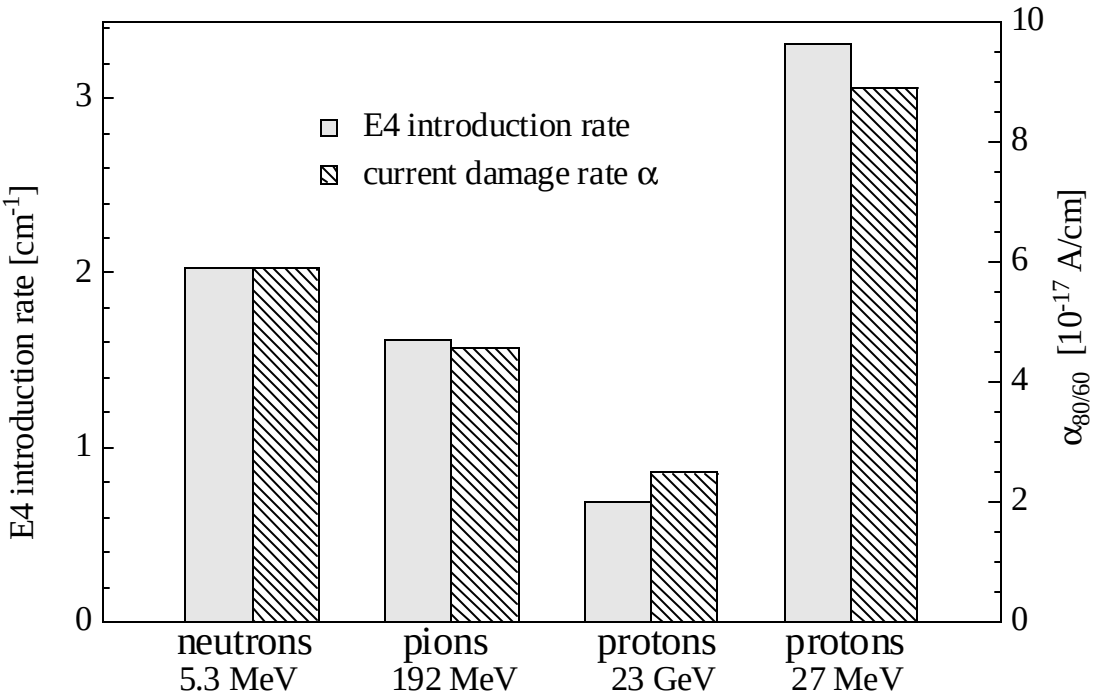

Fig. 11. Correlation between defect level E4 and the α value.

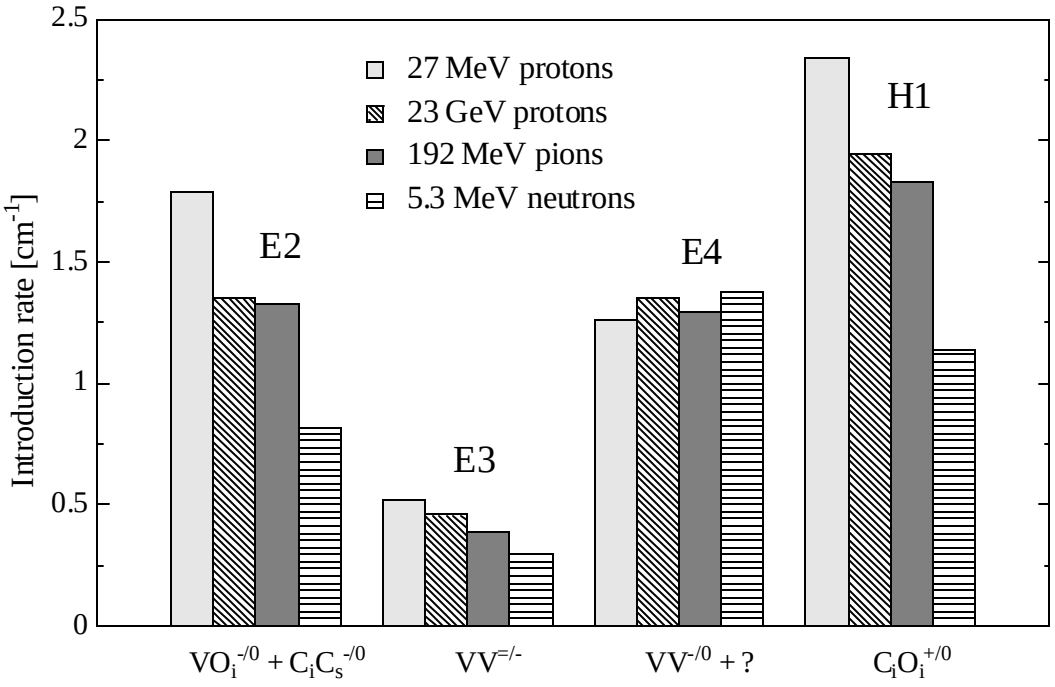

Fig.12.: Particle dependent introduction rate of defects E2, E3, E4 and H1.